Chemical Engineering Journal 156 (2010) 487–495

Contents lists available at ScienceDirect

Chemical Engineering Journal

journal homepage: www.elsevier.com/locate/cej

Polymeric nanofibers containing solid nanoparticles prepared by electrospinning and their applications

Nasser A.M. Barakat[a,b,*], M.F. Abadir[c], Faheem A. Sheikh[d], Muzafar A. Kanjwal[e], Soo Jin Park[b], Hak Yong Kim[f,*]

[a] Chemical Engineering Department, Faculty of Engineering, El-Minia University, El-Minia, Egypt
[b] Center for Healthcare Technology Development, Chonbuk National University, Jeonju 561-756, Republic of Korea
[c] The Chemical Engineering Department, Faculty of Engineering, Cairo University, Cairo, Egypt
[d] Bionano System Engineering Chonbuk National University, Jeonju 561-756, Republic of Korea
[e] Department of Polymer Nano Science and Technology, Chonbuk National University, Jeonju 561-756, Republic of Korea
[f] Department of Textile Engineering, Chonbuk National University, Jeonju 561-756, Republic of Korea

ARTICLE INFO

Article history:
Received 7 July 2009
Received in revised form 9 November 2009
Accepted 12 November 2009

Keywords:
Electrospinning
Colloidal solutions
Metal-doped nanofibers
Nanofibers

ABSTRACT

Generally, polymer solution or sol–gel is used to produce electrospun nanofibers via the electrospinning technique. In the utilized sol–gel, the metallic precursor should be soluble in a proper solvent since it has to hydrolyze and polycondensate in the final solution; this strategy straitens the applications of the electrospinning process and limits the category of the electrospinnable materials. In this study, we are discussing electrospinning of a colloidal solution process as an alternative strategy. We have utilized many solid nanopowders and different polymers as well. All the examined colloids have been successfully electrospun. According to the SEM and FE SEM analyses for the obtained nanofiber mats, the polymeric nanofibers could imprison the small nanoparticles; however, the big size ones were observed attaching the nanofiber mats. Successfully, the proposed strategy could be exploited to prepare polymeric nanofibers incorporating metal nanoparticles which might have interesting properties compared with the pristine. For instance, PCL/Ti nanofiber mats exhibited good bioactivity compared with pristine PCL. The proposed strategy can be considered as an innovated methodology to prepare a new class of the electrospun nanofiber mats which cannot be obtained by the conventional electrospinning technique.

1. Introduction

The past decades have witnessed tremendous progress in the development of the electrospinning technique to widen the applications of the obtained products. Simplicity of the electrospinning process, the diversity of the electrospinnable materials, and the unique features of the obtained electrospun nanofibers provide especial interest for both of the technique and resultant products. However, many technical issues still need to be resolved before electrospinning process becomes more popular and the electrospun nanofibers get strength for industrial level applications. Some researchers have reported modifications of this technique to enhance the alignment of the produced nanofibers [1–7]. Others have focused on the morphology of the obtained nanofibers; they have improved the technique to produce nanofibers with especial features [8–11]. In all the previous studies, the researchers have either modified the electrospinning instrumental design or especially treated the resultant product.

Generally, the electrospun solution is either polymer(s) dissolved in proper solvent or metallic precursor/polymer solution. The distinct feature of these solutions is that they have to be completely miscible. In other words, in case of adding metallic precursor, it should be soluble in a suitable solvent since it has to hydrolyze and polycondensate in the final precursor/polymer mixture to form the gel network. Actually, this strategy fettered the applications of the electrospinning process. In this study, we are introducing electrospinning of a colloidal solution as a new strategy to broaden the category of electrospinnable materials. The utilized solutions in this study were composed of solid nanoparticles/polymer colloid; the invoked solid materials have been chosen to be insoluble in the solution. Different solid metallic precursor and polymers have been used to properly genarlize the proposed strategy. The obtained results were satisfactory.

* Corresponding author at: Center for Healthcare Technology Development, Chonbuk National University, Jeonju 561-756, Republic of Korea.
Tel.: +82 63 270 2351, fax: +82 63 270 2348.
E-mail addresses: nasbarakat@yahoo.com (N.A.M. Barakat), khy@chonbuk.ac.kr (H.Y. Kim).

1385-8947/$ – see front matter © 2009 Elsevier B.V. All rights reserved.
doi:10.1016/j.cej.2009.11.018

2. Experimental details

2.1. Materials

Different polymers have been used in this study: poly(vinyl alcohol) (PVA, molecular weight (MW = 65,000 g/mol, Dong Yang Chem. Co., South Korea), poly(ε-caprolactone) (PCL, MW = 80,000, Aldrich), polyurethane (PU, MW = 110,000, medical grade, Cardio Tech. Intern., Japan), poly(L-lactide) (PLLA, MW = 650,000, Boeringer Ingelheim, Germany) and poly(vinyl acetate) (PVAc, MW = 500,000 g/mol, Aldrich Co., USA). Also, different solid nanopowders have been added to the polymer solutions; silver acetate (Ag(OAc), 99.9%, assay, Showa Co., Japan), boron nitride (BN, 99% assay, average particle size >40 nm, Showa Co., Japan), calcined bovine bone and pure metal nanoparticles (titanium, cobalt and zinc) which were obtained from NaBond Tech. Co. Ltd., Shenzhen, P.R. China.

2.2. Experimental work

A colloidal solution was prepared by mixing the solid powder with the polymer solution and stirring over night. The obtained solution was placed in a plastic capillary. A copper or carbon pin connected to a high-voltage generator was inserted in the solution, and the solution was kept in the capillary by adjusting the inclination angle. A ground iron drum covered by polyethylene sheet was serving as a counter-electrode. For all the utilized polymer/solid nanoparticles, colloids have been electrospun at almost the same working parameters, i.e. 20 kV voltage, 15 cm distance between the needle and the cylindrical collector, normal syringe (no feeding pump) has been invoked. Scheme 1 shows a conceptual illustration for the utilized electrospinning instrument. Moreover, all the formed nanofiber mats were dried for 24 h under vacuum. During the drying process, suction pump was running to suck any vapor in the drying champer. Therefore, the dried nanofiber mats did not have any solvent residual.

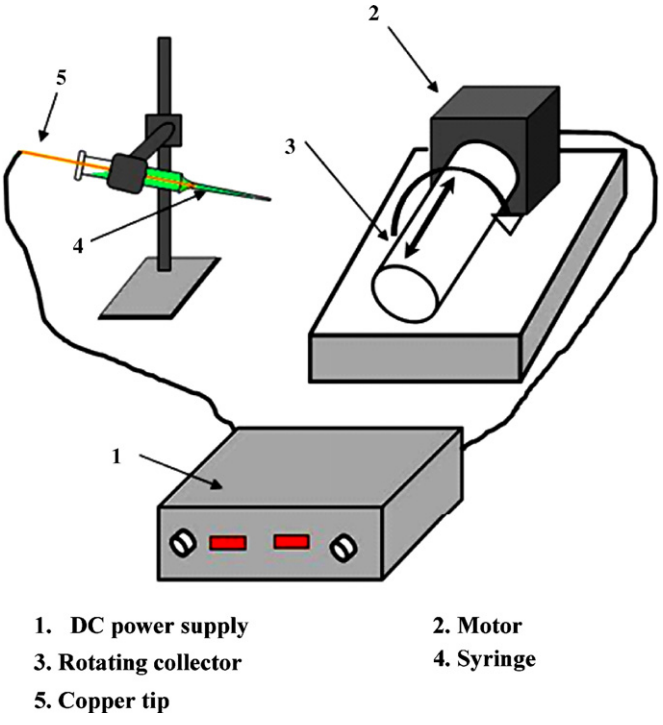

Scheme 1. Schematic diagram for a simple electrospinning spinning apparatus: (1) DC power supply, (2) motor, (3) rotating collector, (4) syringe and (5) copper tip.

2.3. Characterization

Surface morphology was studied by a scanning electron microscope (SEM, JSM-5900, JEOL, Japan) and a field emission scanning electron microscope (FESEM, Hitachi S-7400, Hitachi, Japan) equipped with energy dispersive X-ray (EDX). Hydrodynamic particles size and size distribution of the colloidal solution were determined by a dynamic light scattering (DLS) (Malvern System 4700 instrument, Otsuka Electronics Co., USA) equipped with a vertically polarized light supplied by an argon-ion laser (Cyonics) operated at 20 mW. All experiments were performed at room temperature with measuring angle of 90° to the incident beam. Surface charge ζ potential of the NPs was determined with an electrophoretic light scattering (ELS) measurement by (ELS 8000/6000 Otsuka Electronics Co., Japan) at room temperature with a measuring angle of 20° when compared to the incident beam. Spectroscopic characterization has been investigated by a Fourier-transform infrared (FT-IR), the spectra were recorded as KBr pellets using Varian FTS 1000 FT-IR, Mid-IR spectral range, cooled DTGS detector, Scimitar series, Varian Inc., Australia. Information about the phases and crystallinity was obtained by using Rigaku X-ray diffractometer (XRD, Rigaku Co., Japan) with Cu Kα (λ = 1.540 Å) radiation over suitable range of Bragg angle.

3. Results and discussion

The electrospinning technique involves the use of a high voltage to charge the surface of a polymer solution droplet and thus to induce the ejection of a liquid jet through a spinneret. Due to bending instability, the jet is subsequently stretched by many times to form continuous, ultrathin fibers. Therefore, the process is carried out for electric conductive solutions. Consequently, the electrospinning is widely used for the production of many polymeric nanofibers. Moreover, the elctrospinning have been exploited to produce metal oxides [12] or pure metal nanofibers [13–16] by calcination of electrospun mats obtained from completely miscible sol–gel solutions. However, we are introducing electrospinning of colloidal solutions, different solid nanopowders and polymers as well have been utilized. Electrospinning of colloidal solution can be conceptually illustrated in Scheme 2. As shown in this scheme, the colloidal solution might have solid nanoparticles with different sizes. During the electrospinning process, the particles having diameter less than the diameter of the polymeric nanofibers will be imprisoned inside the nanofibers. Actually, we think that the incorporation process might depend on the surface tension of the polymer solution and the wettability between the solid particle and the polymer solution. In other words, high surface tension and good wettability reveal well imprisoning of the small nanoparticles. However, the big particles will stick on the polymeric nanofibers.

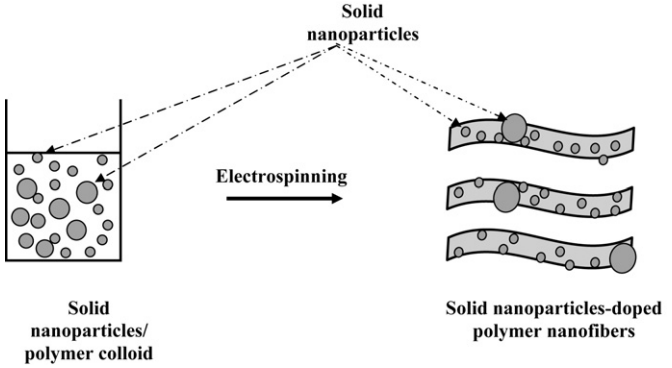

Scheme 2. Conceptual illustration showing electrospinning of the colloidal solution.

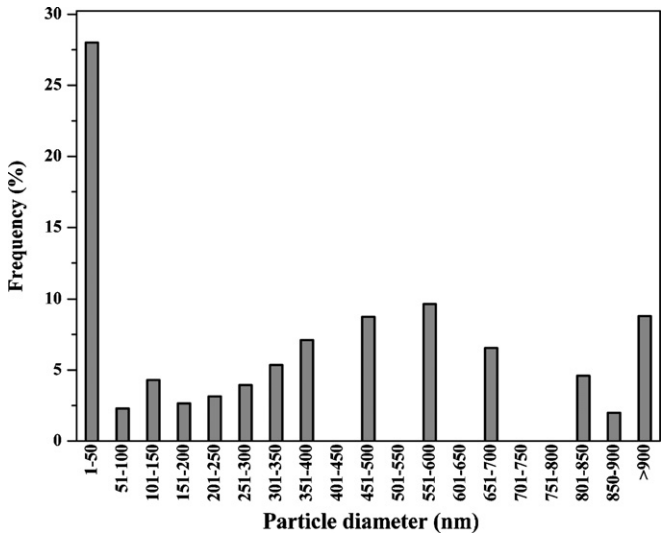

Fig. 1. Silver acetate particles size distribution in PVA solution.

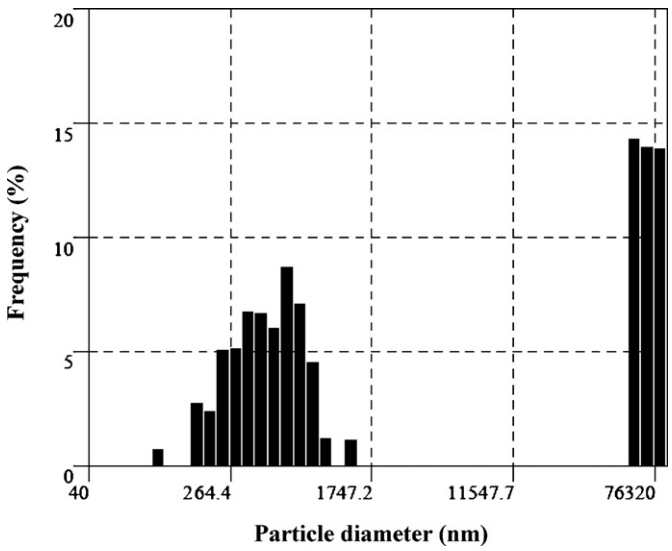

Fig. 2. DLS results for silver acetate particles size distribution in water.

3.1. Silver acetate/PVA colloid

Silver acetate (AgAc) is not soluble in water and many other common solvents. Accordingly, mixing of AgAc powder with PVA aqueous revealed to produce colloidal solution. Typically, a colloidal solution was prepared by mixing 0.5 g AgAc with 7 g PVA aqueous solution (10 wt%) and stirring over night. The obtained solution was yellowish in color, but, it was stable (i.e. there was no precipitation in the syringe during the electrospinning). To precisely investigate the characteristics of the prepared colloidal solution, measurement of the average hydrodynamic diameter and the particle size distribution have been performed using DLS analysis. Fig. 1 demonstrates the particle size distribution obtained. As shown in this figure, many particles (~21%) have very small size (less than 50 nm). According to these results, the average diameter of the AgAc in the utilized colloidal solution was 279 ± 2 nm. Zeta (ζ) potential is the most common measured parameter characterizing the colloidal solutions [17]. For AgAc/PVA colloidal solution the measured ζ potential was -2.1 mV. It is noteworthy mentioning that the DLS analysis has been conducted in AgAc/H_2O solution to investigate the particles size of the pristine AgAc. As shown in Fig. 2, the obtained results indicate that the sizes of the pristine AgAc particles are higher than in case of incorporation in PVA solution. Accordingly, to explain this phenomenon we can say that with long stirring time and high viscosity of the polymer solution, the AgAc particles were grinded and attached in the polymeric chains. Considering the acetate group is slightly polar, a weak hydrogen bond between the particles and the polymer series might be also suggested. Moreover, the small particles could be imprisoned inside the polymeric chain. As a long stirring time in preparation of the polymer solution (several days) was utilized, the large portion which has small size (1–50 nm) might be considered as AgAc particles. Fig. 3 shows the SEM and FESEM images of the AgAc/PVA dried nanofiber. As shown in Fig. 3A which demonstrates the SEM images of the dried AgAc/PVA nanofiber mats, the electrospinning process produced relatively smooth nanofibers. Beads or agglomerated nanofibers cannot be observed in the obtained mats. Fig. 3B represents FESEM image, as can be seen in this figure, the colloidal solution has produced smooth and well morphology nanofibers with wide diameter range. An astute scrutiny in Fig. 3B results in observing some silver acetate nanoparticles. These nanoparticles are very few and so small in size, so, we can say the majority of the silver acetate nanoparticles are imprisoned inside the PVA nanofibers. As shown in Fig. 1, large portion of AgAc particles has small particle size. Detailed DLS indicated that in this portion the small particles are abundant. Therefore, the apparent particles in Fig. 3B can be confidently explained as AgAc have not been involved inside the PVA nanofibers.

To ensure that the AgAc particles were not reacted or hydrolyzed during/after the electrospinning process, FT-IR analysis was carried out. It is note worthy mentioning that according to the composition of the used colloidal solution and the molecular weights of AgAc and PVA, the molar ratio of hydroxyl to acetate groups in the mixture is almost 52:1. Therefore, if any reaction takes place between these two groups; acetate anions will completely disappear from the mixture. Moreover, if acetate anions hydrolyze in the solution this will

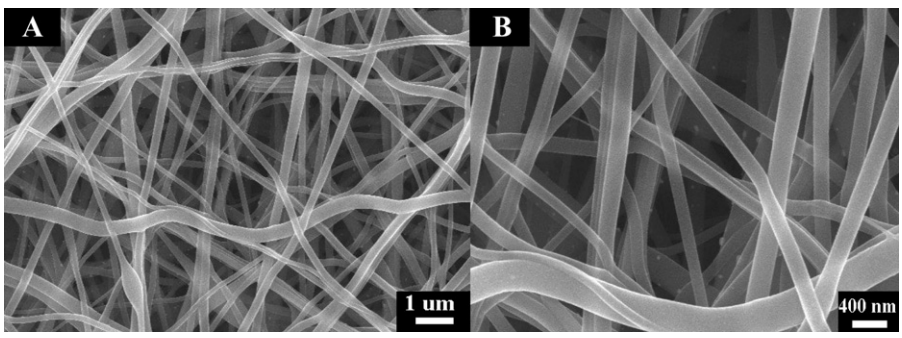

Fig. 3. Scanning electron microscope (SEM) and field emission electron microscope (FE SEM) images for silver acetate/PVA dried nanofiber mats.

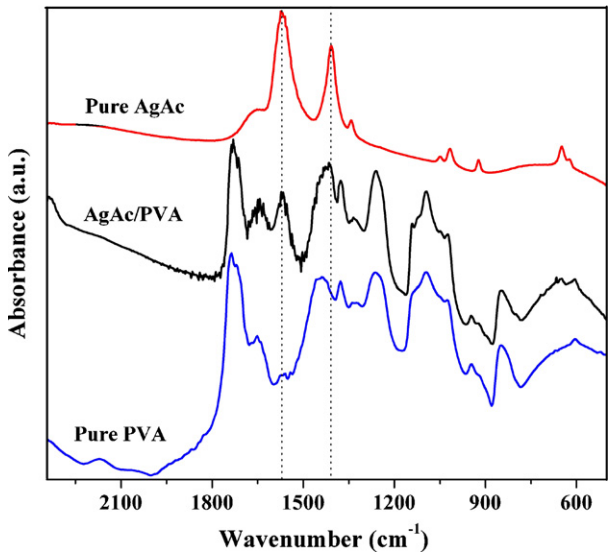

Fig. 4. FT-IR spectra for pure silver acetate, pristine PVA and silver acetate/PVA electrospun nanofiber mats; the dashed lines demonstrate the location of the peaks representing the acetate ion.

lead to from acetic acid which will evaporate during the drying step. Fig. 4 shows the FT-IR results for the utilized silver acetate, the pristine PVA, and the electrospun nanofiber mats. As shown in this figure, the characteristics absorption bands of the acetate anion which appear from 1590 to 600 cm^{-1} [18,19] can be observed in the AgAc and the nanofiber mats spectra. Within this range, two main peaks at 1570 and 1408 cm^{-1} are clearly seen in the nanofiber mats and the pure AgAc spectra, no similar peaks at the same wavenumbers can be observed in the pristine PVA spectra. Moreover, all the other small peaks denoting the acetate group can be noticed in the electrospun mat spectra. Furthermore, the main molecular structure of PVA was not affected since all the peaks of PVA exist in the electrospun mat spectra. These results indicate that AgAc particles in the electrospun colloidal solution were not affected and the obtained electrospun PVA nanofibers imprison the AgAc particles. However, a limited reduction in AgAc took place since PVA does have reduction power [20,21], so the observed yellowish color of the AgAc/PVA colloid might explained as a partial decomposition of AgAc into Ag nanoparticles.

3.2. Boron nitride/PVA colloid

Boron nitride (BN) is a binary compound of boron and nitrogen, especially a white, fluffy powder with high chemical and thermal stability, and high electrical resistance, moreover it has wide applications [22]. Boron and nitrogen are neighbours of carbon in the periodic table, in combination boron and nitrogen have the same number of outer shell electrons. The atomic radii of boron and nitrogen are similar to that of carbon. It is not surprising therefore that boron nitride and carbon exhibit similarity in their crystal structure and most of the physical and chemical properties. Therefore, BN is not soluble in many common solvents; especially water. A mixture of BN and the aqueous PVA formed a stable colloid, zeta potential values were −8.53, −5.18, −3.73 and −3 eV for BN/PVA colloids with compositions of 2, 7, 10 and 15 wt% (with respect to PVA solution), respectively. The negative sign and the higher absolute value of zeta potential reflect the stability of the prepared colloids. It is noteworthy mentioning that DLS analysis has been conducted on BN/water solution to measure the size of the utilized BN powder, the average size of the particles was 347 nm. Moreover, considerable portion has small size. Fig. 5 shows SEM images for the dried nanofiber mats of 2 and 7% colloidal solutions. As shown in the figure, the 2% electrospun mats almost free from the BN nanoparticles (Fig. 5A and B) which means that majority of the particles are imprisoned inside the nanofibers. However, for the 7% mat, some particles can be observed attached with the nanofibers surfaces (Fig. 5C and D).

3.3. Metal nanopowders/polymer colloids

Incorporation of metal nanoparticles in the polymeric nanofiber mats is desirably demand since the metal nanoparticles provide

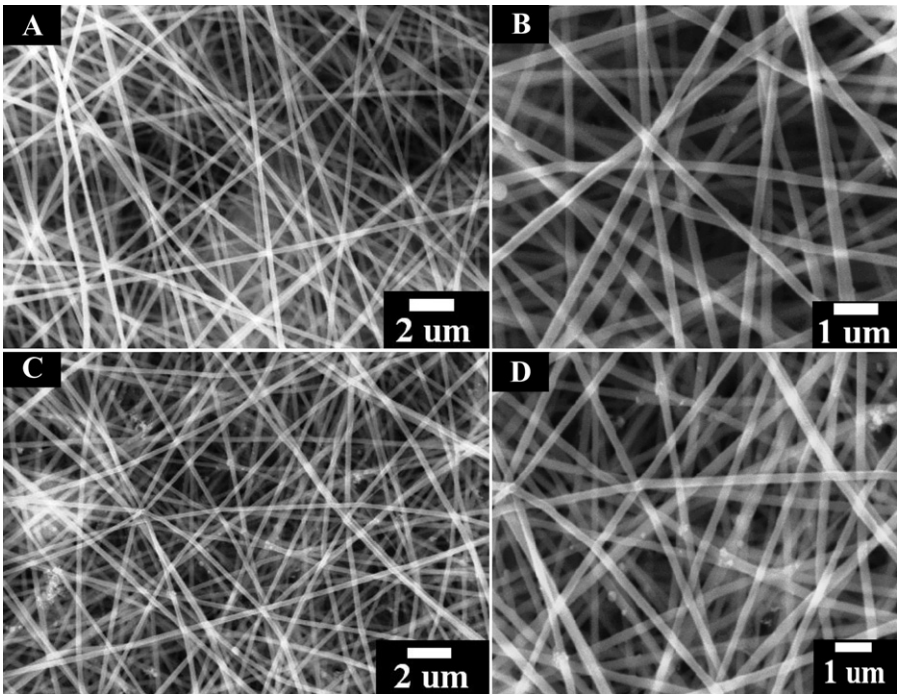

Fig. 5. Scanning electron microscope (SEM) images for 2 wt% (A) and (B) and 7 wt% (C) and (D) boron nitride/PVA dried nanofiber mats.

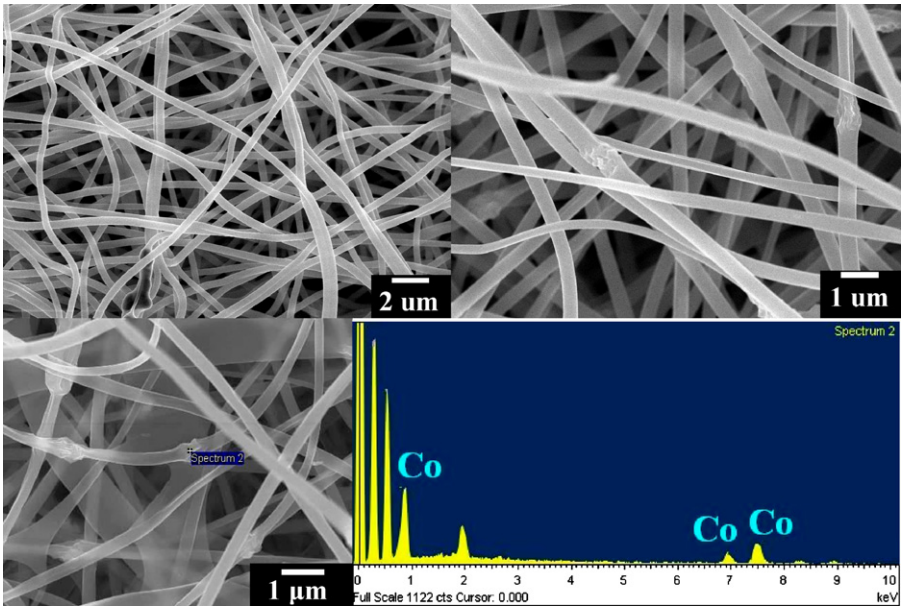

Fig. 6. Scanning electron microscope (SEM) images; (up) and EDX results; (down) for Co nanopowder/PVA nanofiber mats.

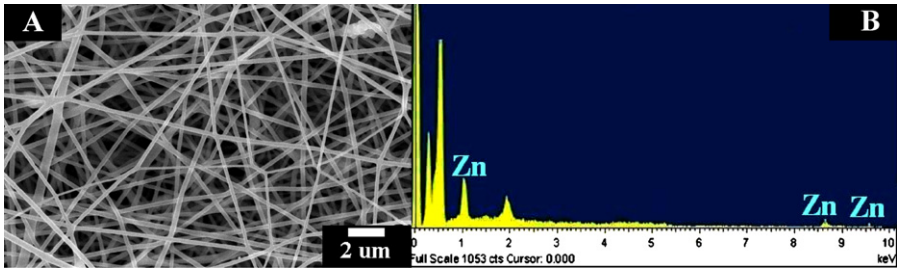

Fig. 7. Scanning electron microscope (SEM) images (A) and EDX results (B) for Zn nanopowder/PVAc nanofiber mats.

the polymer nanofibers new characteristics. As the metals powders are insoluble in any solvent, all the reported metal/polymer electrospun nanofiber mats contain metal compounds rather than zero-oxidation state metal nanoparticles. In other words, a metal precursor had to be used as a source of metal. Converting the metal ions present in the metal precursor into metal molecules always needs strong reducing agents (especially in case of active metals) which definitely affect the chemical composition of the polymers. Therefore, according to our best knowledge, only noble metals (Ag and Pt) nanoparticles could be successfully incorporated in polymeric nanofibers [23,24]. Electrospinning of colloid might be an interesting solution for this dilemma as metal nanopowder can be used. In this study, we have successfully electrospun metal nanopowder/polymer solution mixtures. Fig. 6 (up) shows the SEM images of a nanofiber mat composed of cobalt nanopowder/PVA, solid content in the original colloid was 5 wt%. As shown in this figure, well morphology nanofibers could be obtained. To assure that the cobalt nanoparticles have been incorporated in the PVA nanofibers, EDX analysis has been performed, the obtained results were satisfactory as shown in Fig. 6 (down) as the cobalt peaks are apparent. It is worthy mentioning that the utilized cobalt powder has an average particle size of ~50 nm that is why no particles could be observed in SEM or FE SEM images (Fig. 6) since all particles are imprisoned inside the nanofibers as the average nanofibers diameter is much greater than the nanoparticles size.

For generalization, different polymer and metal nanopowder have been utilized. Fig. 7 shows the SEM image and EDX analysis results for an electrospun nanofiber mat obtained from a colloid

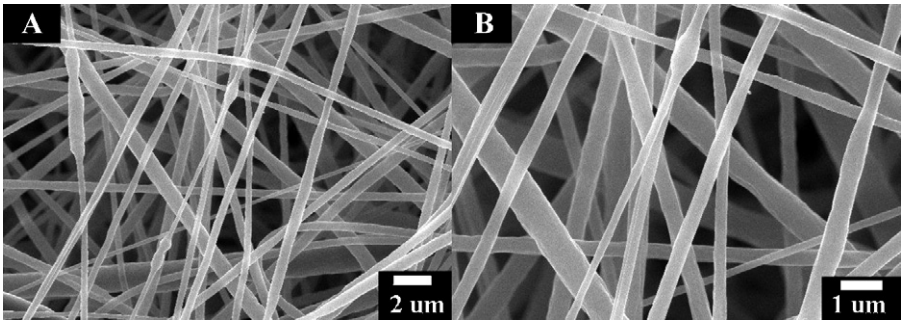

Fig. 8. Field emission scanning electron microscope (FE SEM) images for Ti/PCL electrospun nanofiber mats in low (A) and high (B) magnifications.

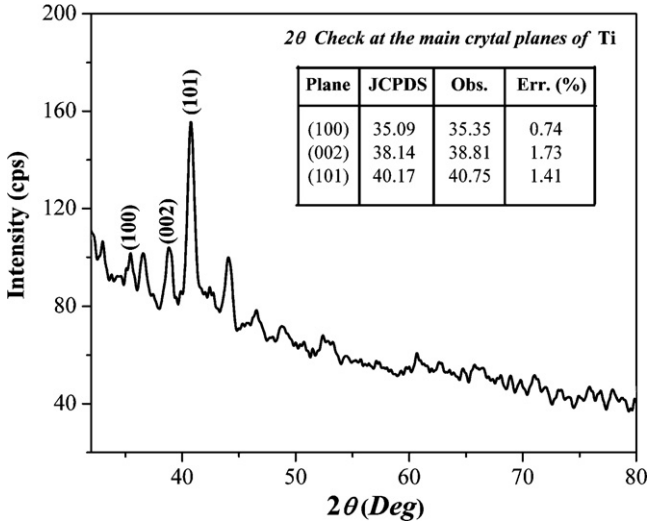

Fig. 9. XRD results for PCL/Ti nanopowder electrospun nanofiber mats. The inset table shows comparison of the 2θ values at the main three peaks of the standard titanium and the observed values. (Abbreviations in the table—Plane: the crystal plane, JCPDS: the standard value according to JCPDS data base, Obs.: the observed value from the spectra and Err.: the percentage error).

composed of zinc nanopowder (particle size <50 nm) and poly (vinyl acetate) (solid content 5 wt%). According to the EDX results, one can claim that the proposed strategy successes to produce PVAc nanofibers embedding zinc nanoparticles.

3.4. Metal nanopowder/polymer for biological applications

Poly(ε-caprolactone) (PCL) was successfully utilized as hard tissue scaffold because of its proved biocompatibility [25–27] and processability properties [28]. Because titanium is a light and corrosion resistant metal, it caught the attention of many scientists, who sought to use it pure or to obtain alloys and was employed successfully in the aerospace, military and chemical industries. These characteristics raised the hypothesis that the material could be used as implant materials since it is biologically safe [29,30]. It is noteworthy mentioning that the large surface area of the nanofibers and the high porosity of the electrospun nanofiber mats make the later good candidates for hard tissue engineering purposes if the biological constraints are satisfied. Therefore, combination of these two interesting biomaterials in single nanofiber mats might have good application in the biomedical fields. In this study titanium powder (particle size <100 nm) and PCL solution (10 wt%, in two solvents mixture; methyl chloride and *N*,*N*-dimethylformamide with weight ratio of 3:17) have been well mixed and electrospun. The

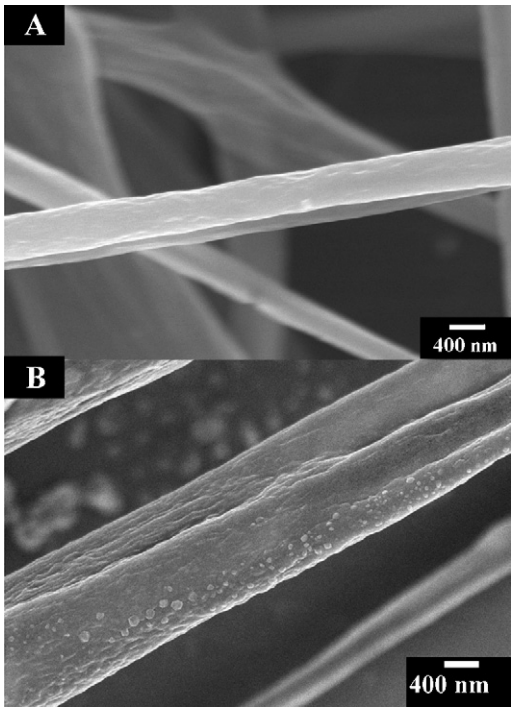

Fig. 11. FE SEM images for Ti-free PLLA (A) and Ti-doped PLLA and (B) nanofibers.

final colloid was having titanium weight percentage of 2%. Fig. 8 shows the FE SEM of the obtained nanofiber mats, as shown in this figure well morphology nanofiber could be obtained. To ensure that the produced electrospun mats embed the added titanium nanoparticles, we have utilized XRD analysis. Fig. 9 shows the XRD results for the obtained electrospun PCL/Ti nanofiber mats. As shown in this figure and the present inset table, the main peaks of titanium can be clearly observed with very small percentage errors compared with the standard titanium (JCPDS 44-1294). XRD data affirmed incorporation of the titanium nanopowders in the PCL nanofiber mats.

To check the advantage of incorporating titanium nanoparticles in PCL nanofibers, we have examined the *in vitro* bioactivity of both of pristine PCL and PCL/Ti nanofiber mats. The *in vitro* bioactivity study was done by using simulated body fluid solution (SBF) prepared by using previously described method elsewhere [31]. The salt components viz. NaCl, $NaHCO_3$, KCl, K_2HPO_4, $MgCl_2$, $6H_2O$, HCl, $CaCl_2$, Na_2SO_4, and $(CH_2OH)_3CNH_2$ were added in the same propositions as described in the reference to give the ionic concentration of human plasma. The pH of the ionic buffer was adjusted to 7.4 by adding 0.1 M HCl or 0.1 M NaOH. Briefly, PCL and PCL/Ti nanofiber

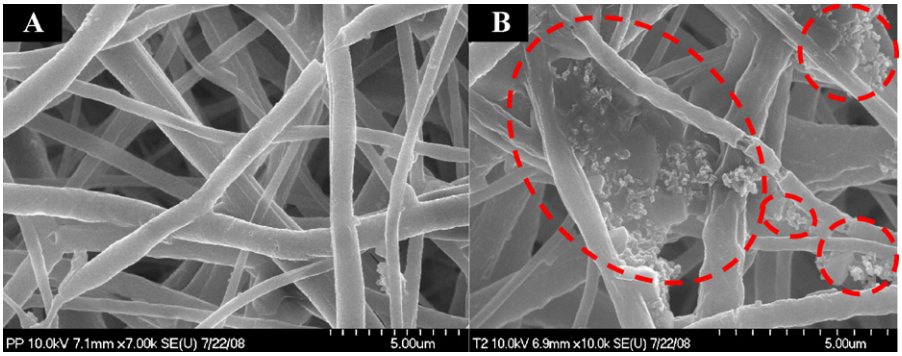

Fig. 10. Field emission scanning electron microscope (FE SEM) images for PCL (A) and PCL/Ti (B) electrospun nanofibers after soaking in the SBF for 10 days. The red shapes point to the precipitated apatite-like materials.

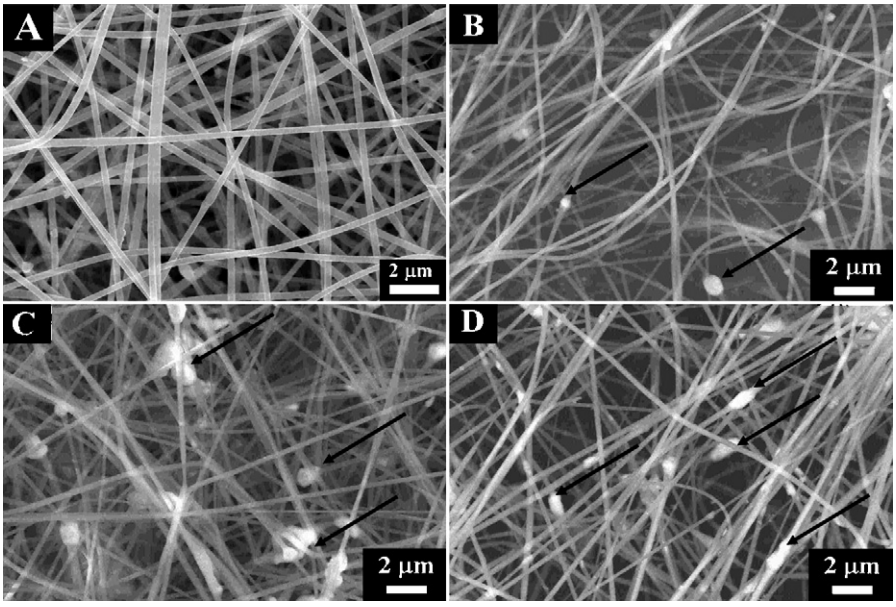

Fig. 12. SEM image for pristine PVA (A) and PVA/HAp electrospun nanofiber mats containing: 3 wt% (B), 5 wt% (C) and 7 wt% (D) HAp with respect to polymer solution. The arrows point to HAp nanoparticles.

mats were soaked in the SBF for time period of 10 days in plastic vials to investigate the formation of the bone-like apatite on the mats surfaces. After the soaking time, both mats have been subjected to FE SEM analysis; the results are demonstrated in Fig. 10. It can be concluded from Fig. 10A that the pristine PCL nanofibers cannot be utilized as hard tissue since no apatite-like materials were precipitated within 10 days. However as can be deduced from Fig. 10B, incorporation of Ti nanoparticles has strongly activated precipitation of the hydroxyapatite on the nanofibers mats which recommends utilizing the prepared PCL/Ti mats the medical fields as both of PCL and Ti are biologically safe as aforementioned.

With the same strategy, poly (L-lactide) (PLLA) and titanium nanopowder colloid have been electrospun. Fig. 11 shows the FE SEM images for pristine PLLA and Ti-doped, panels A and B, respectively. As shown in these images some Ti nanoparticles could be observed in panel B, however, the surface of the pristine polymer is smooth. As PLLA can also be considered as biomaterial, the prepared PLLA/Ti nanofiber mats might have good biological applications.

3.5. Hydroxyapatite/polymer colloid

Hydroxyapatite (HAp) is widely utilized in medical fields, due to its good biocompatibility, bioactivity, high osteoconductive and/or osteoinductive nontoxicity, noninflammatory behavior and nonimmunogenicity properties [32,33]. To produce biologically preferable HAp and avoiding the sophisticated procedures used in the synthesizing of HAp, some researchers have turned into extraction of natural HAp from bio-wastes (usually via calcination). Extraction of HAp from the bio-wastes is biologically safe (no foreign chemicals are utilized) and economically desirable process especially with increasing the world demand of HAp bioceramics. In this study a HAp which can be extracted from the bovine bone [34] was used a solid constituent to prepare HAp/PVA colloid. In this case, proper amounts of 9 wt% PVA (in water) and HAp obtained from calcination of the bovine bones were mixed to prepare colloids contain 0, 3, 5 and 7 wt% HAp with respect to the polymer solutions. SEM images for the obtained nanofiber mats are presented in Fig. 12. As shown, in this figure, some HAp particles can be observed. Actually, obtaining external nanoparticles is due to the large particle size of the prepared HAp compared with

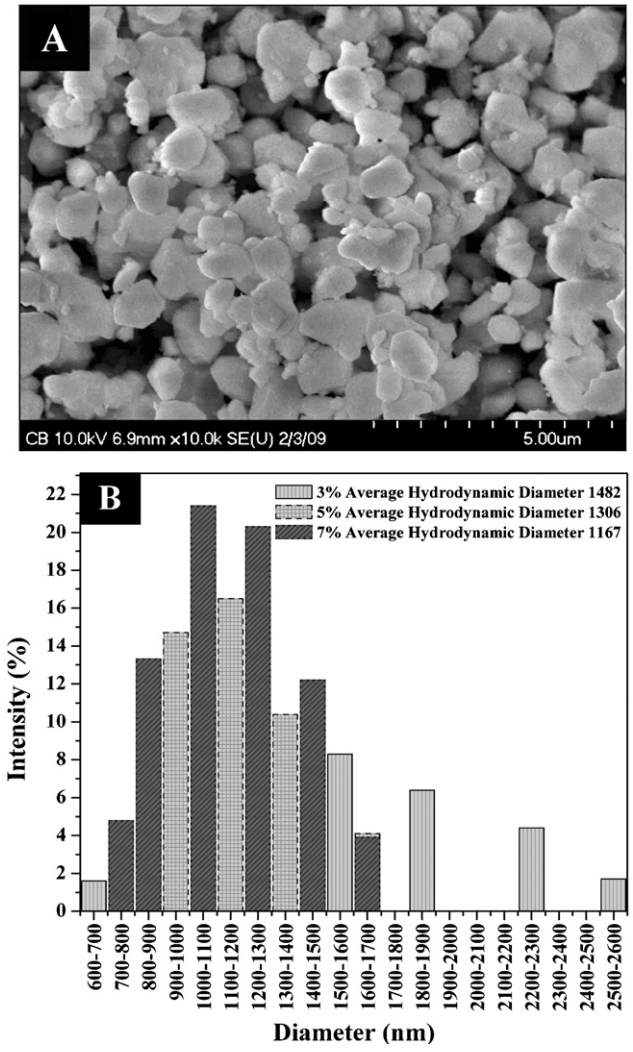

Fig. 13. FE SEM of the calcined bovine bone (A) and particle size distribution of the HAp/PVA colloids (B).

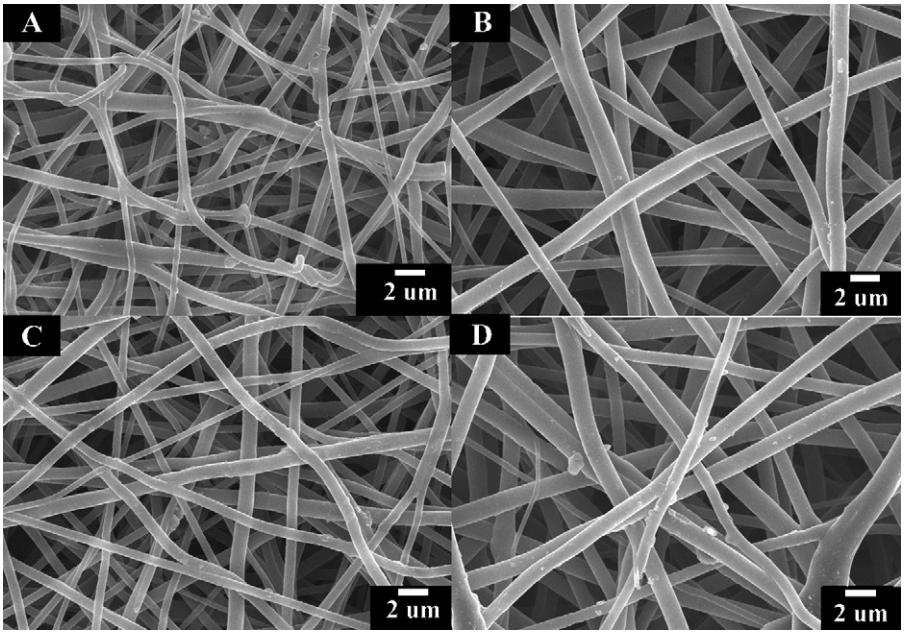

Fig. 14. SEM image for pristine PU (A) and PU/HAp electrospun nanofiber mats containing: 3 wt% (B), 5 wt% (C) and 7 wt% (D) HAp with respect to polymer solution.

PVA nanofibers. The utilized bovine bone has been grinded before calcination, however the particle size of the calcined bone could not be brought into nanoscale. Fig. 13A reveals the FE SEM of the calcined bovine bone, as shown in this figure; the particle size is relatively big. The average particle size in the HAp/PVA colloids has been precisely estimated by using the DLS analysis. The hydrodynamic size distributions of all the prepared colloidal solutions are indicated in Fig. 13B. According to this figure, the average particle diameter of the colloids containing 3, 5 and 7 wt% HAp is 1482, 1306 and 1167 nm, respectively, which provides an explanation of presence of the large HAp nanoparticles in the SEM images (Fig. 12). Moreover, we have measured ζ potential for the HAp/PVA colloidal solutions to assure that the large particles size did not affect the stability of the colloid, the obtained results were satisfactory since ζ potential for the colloids containing 3, 5 and 7 wt% HAp were -14 ± 2, -8 ± 1 and -4 ± 1 mV, respectively.

Poly(urethane) (PU) is thermoplastic, excellent mechanical properties and water insoluble polymer, moreover, it can be used as biomaterial. As nanofibrous morphology strongly modifies the characteristics of any material, these polymer nanofibers have tremendous applications in various fields: biosensors, protective cloths, and epithelial enhancing material [35–37]. Moreover, there are some articles concluded that PU nanofibers can be used as antimicrobial agent [38,39]. Accordingly, improvement of the physiochemical properties of the PU nanofibers by incorporating solid nanoparticles might have good applications. In this study, we have prepared PU/HAp nanofiber mats with different solid contents, however, other solid nanoparticles can also be utilized, HAp has been selected because it is the largest particle size among the solid powders used in this study. Fig. 13A reveals the FE SEM image of the utilized HAp obtained from calcination of the bovine bone. Pristine PU solution (10 wt%) was prepared by stepwise dissolving in tetrahydrofuran (THF) and *N*,*N*-dimethylformamide (DMF). Initially, PU pellets were overnight dissolved in THF after that DMF was added to produce final solution containing 10 wt% of PU in THF/DMF (1:1, w/w). Later on, HAp powders have been mixed with PU solutions to prepare colloids containing solid contents of 3, 5 and 7 wt% with respect to polymer. To precisely estimate the average particle size inside the prepared colloids the hydraulic diameters have been estimated, the results are demonstrated in Fig. 13B. As shown in this figure, the average particle sizes are high for all formulations. The pristine solution and the colloids have been successfully electrospun. Fig. 14 reveals the FE SEM results. PU nanofibers are quit large compared with the PVA nanofibers, so PU nanofibers almost encompassed all the HAp particles in all combinations as shown in Fig. 14. XRD analysis has been carried out to affirm that the nanofibers obtained from the colloids involve HAp particles, the results are presents in Fig. 15. Moreover, to precisely identify the apparent peaks, XRD spectra of the utilized calcined bone and the pristine PU have been included. As shown in this figure, the HAp peaks are clearly apparent in all nanofiber mats obtained from the colloids. These apparent peaks cannot be observed in the pristine PU spectra; moreover, they match the corresponding peaks of the calcined bovine bone as well as the standard peaks of the HAp (JCPDS card no. 09-0432).

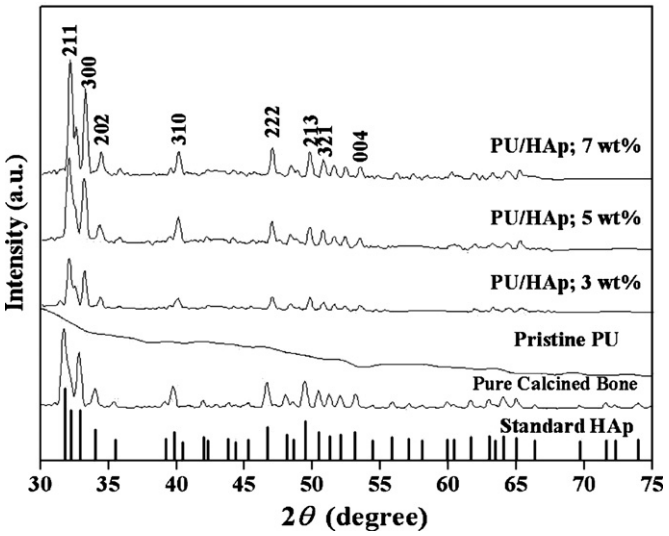

Fig. 15. XRD results for the PU/HAp nanofiber mats containing 0, 3, 5 and 7 wt% HAp powder with respect to the polymer solution. Also, the results for the calcined bovine bone are demonstrated. The bars at the base of the figure represent the location and the relative intensities of the standard HAp (JCPDS card no. 09-0432).

4. Conclusion

In summary, we can say that electrospinning of colloidal solution is valid and the process does not affect the chemical composition of either solid nanoparticles or the utilized polymer. Moreover, some solid nanoparticles might be embedded inside the polymeric nanofibers and others attached on the nanofibers surface according to the particle size. Electrospinning of the colloidal solution could be considered as a simple and effective solution to produce metal/polymer electrospun nanofiber mats which might have interesting biological and other properties according to the utilized metal nanopowder and polymer. Finally, we can claim that electrospinning of colloidal solution is opening a new avenue in the field of electrospinning technology.

Acknowledgements

This work was supported by the grant of the Korean Ministry of Education, Science and Technology (The Regional Core Research Program/Center for Healthcare Technology & Development, Chonbuk National University, Jeonju 561-756 Republic of Korea). We thank Mr. T.S. Bae and J.C. Lim, KBSI, Jeonju branch, and Mr. Jong-Gyun Kang, Centre for University Research Facility, for taking high-quality FESEM and TEM images, respectively.

References

[1] D. Li, Y. Wang, Y. Xia, Adv. Mater. 16 (2004) 361–366.
[2] E. Smit, U. Bűttner, R.D. Sanderson, Polymer 46 (2005) 2419–2423.
[3] J. Doshi, D.H. Reneker, J Electrostat 35 (1995) 151–160.
[4] E. Zussmann, A. Theron, A.L. Yarin, Appl. Phys. Lett. 82 (2003) 973–975.
[5] A. Bournat, US Patent, 4,689,186, 1987.
[6] J.M. Deitzel, J.D. Kleinmeyer, J.K. Hirvonen, T.N.C. Beck, Polymer 42 (2001) 8163–8170.
[7] H. Fong, L. Weidong, C.S. Wang, R.A. Vaia, Polymer 43 (2002) 775–780.
[8] I.H. Yu, S.V. Fridrikh, G.C. Rutledge, Adv. Mater. 16 (2004) 1562–1566.
[9] D. Li, Y. Xia, Nano Lett. 4 (2004) 933–938.
[10] J.T. McCann, M. Marquez, Y. Xia, Z. Sun, E. Zussman, A.L. Yarin, J.H. Wendorff, A. Geirne, Adv. Mater. 15 (2003) 1929–1932.
[11] M. Wang, H. Singh, T.A. Hatton, G.C. Rutledge, Polymer 45 (2004) 5505–5514.
[12] W. Sigmund, J. Yuh, H. Park, V. Maneeratana, G. Pyrgiotakis, A. Daga, J. Taylor, J.C. Nino, J. Am. Ceram. Soc. 89 (2006) 395–407.
[13] W. Hui, Z. Rui, L. Xinxin, L. Dandan, P. Wei, Chem. Mater. 9 (2007) 3506–3511.
[14] B. Michael, B. Mathias, G. Martin, M. Werner, H.W. Joachim, S. Andreas, W. Dirk, B. Andre, G. Armin, G. Andreas, Adv. Mater. 18 (2006) 2384–2386.
[15] N.A.M. Barakat, K.D. Woo, M.A. Kanjwal, E.C. Kyung, M.S. Khil, H.Y. Kim, Langmuir 24 (2008) 11982–11987.
[16] N.A.M. Barakat, B. Kim, H.Y. Kim, J. Phys. Chem. C 113 (2009) 531–536.
[17] F.A. Sheikh, N.A.M. Barakat, B.S. Kim, S. Aryal, M.S. Khil, H.Y. Kim, Mater. Sci. Eng. C 29 (2009) 8659–8876.
[18] Y. Jiang, Y. Wu, B. Xie, Y. Xie, Y.T. Qian, Mater. Chem. Phys. 74 (2002) 234–237.
[19] N.A.M. Barakat, M.S. Khil, F.A. Sheikh, H.Y. Kim, J Phys. Chem. C 112 (2008) 12225–12233.
[20] G. Dong, X. Xiao, X. Liu, B. Qian, Z. Ma, S. Ye, D. Chen, J. Qiu, J. Nanoparticles Res., doi:10.1007/s11051-009-9665-3.
[21] G. Dong, X. Liu, X. Xiao, B. Qian, J. Ruan, S. Ye, H. Yang, D. Chen, J. Qiu, Nanotechnology 20 (2009) 055707–055713.
[22] G. Dong, X. Liu, X. Xiao, Q. Zhang, G. Lin, Z. Ma, D. Chen, J. Qiu, Electrochem. Solid State Lett. 12 (2009) K53–K60.
[23] W.J. Jin, H.K. Lee, E.H. Jeong, W.H. Park, J.H. Youk, Macromol. Rapid Commun. 26 (2009) 1903–1907.
[24] K. Mallick, M.J. Witcomb, A. Dinsmore, M.S. Scurrell, Langmuir 21 (2005) 7964–7969.
[25] M.C. Serrano, R. Pagani, M. Vallet-Regi, J. Peňa, P.J. Rámila, I. Izquierdo, M.T. Protolés, Biomaterials 25 (2004) 5603–5611.
[26] H. Sun, L. Mei, C. Song, X. Cui, P. Wang, Biomaterials 27 (2006) 1735–1740.
[27] L. Savarino, N. Baldini, M. Greco, O. Capitani, S. Pinna, S. Valentini, et al., Biomaterials 28 (2007) 3101–3109.
[28] B.Y. Tay, S.X. Zhang, M.H. Myint, F.L. Ng, M. Chandrasekaran, L.K.A. Tan, J. Mater. Process. Technol. 182 (2007) 117–121.
[29] M.A. Khan, R.L. Williams, D.F. Williams, Biomaterials 17 (1996) 2117–2126.
[30] E. Eisenbarth, D. Velten, M. Müller, R. Thull, J. Breme, Biomaterials 25 (2004) 5705–5713.
[31] T. Kokubo, H. Kushitani, S. Sakka, T. Kitsugi, T. Yamamuro, J. Biomed. Mater. Res. 24 (1990) 721–734.
[32] J.C. Elliott, Structure and Chemistry of the Apatites and other Calcium Orthophosphates, Elsevier, Amsterdam, 1994.
[33] S.F. Hulber, J.C. Bokros, L.L. Hench, J. Wilson, G. Heimke, Ceramics in clinical applications: past, present and future, in: P. Vincenzini (Ed.), High Tech Ceramics, Elsevier, Amsterdam, 1987, pp. 189–213.
[34] N.A.M. Barakat, M.S. Khil, A.M. Omran, F.A. Sheikh, H.Y. Kim, J. Mater. Process. Technol. 209 (2009) 3408–3415.
[35] J. Han, H.J.D. Taylor, D.S. Kim, Y.S. Kim, Y.T. Kim, G.S. Cha, H. Nam, Sens. Actuators B 123 (2007) 384–390.
[36] N. Hains, V. Friscic, D. Gordos, Int. J. Cloth. Sci. Technol. 15 (2003) 250–257.
[37] M.S. Khil, D.I. Cha, H.Y. Kim, I.S. Kim, N.J. Bhattarai, Biomed. Mater. Res. B: Appl. Biomater. 67 (2003) 675–679.
[38] C. Yao, X. Li, K.G. Neoh, Z. Shi, E.T. Kang, J. Membr. Sci. 15 (2008) 259–274.
[39] E.H. Jeong, J. Yang, J.H. Youk, Mater. Lett. 61 (2007) 3991–3994.